THE JOURNAL OF PHYSICAL CHEMISTRY B

ARTICLE

pubs.acs.org/JPCB

The Promoting Vibration in Human Heart Lactate Dehydrogenase Is a Preferred Vibrational Channel

Ardy Davarifar,[†] Dimitri Antoniou,[†,‡] and Steven D. Schwartz*[,†,‡,§,∥]

[†]Department of Biophysics and [§]Department of Biochemistry, Albert Einstein College of Medicine, 1300 Morris Park Avenue, Bronx, New York 10461, United States

[‡]Department of Chemistry and Biochemistry, University of Arizona, 1306 East University Boulevard, Tucson, Arizona 85721, United States

[∥]Institut des Hautes Études Scientifiques, 91440 Bures-sur-Yvette, France

ABSTRACT: We examine whether the rate-promoting vibration of lactate dehydrogenase is a preferred axis of thermal energy transfer. While it seems plausible that such a mechanistically important motion is also a favored direction of energy transfer, none of the previous studies of rate-promoting vibrations in enzymatic catalysis have addressed this question. It is equally likely that the promoting vibration, though catalytically important, has no different properties than any other axis in the protein. Resolution of this issue is important for two reasons: First, if energy is transferred along this axis in a preferred fashion, it shows that the protein is engineered in a way that transfers thermal energy into a motion that is coupled to the chemical step. Second, the discovery of a preferred direction of thermal transfer provides a potential route to experimental verification of the promoting vibration concept. Our computational experiments are specifically designed to mimic potential laser experiment with the deposition of thermal energy in an active-site chromophore with subsequent measurement of temperature at various points in the protein. Our results indicate that the promoting vibration is indeed a preferred channel of energy transfer. In addition, we study the vibrational structure of the protein via the dynamical structure factor to show preferred vibrational motion along the promoting vibration axis is an inherent property of the protein structure via thermal fluctuations.

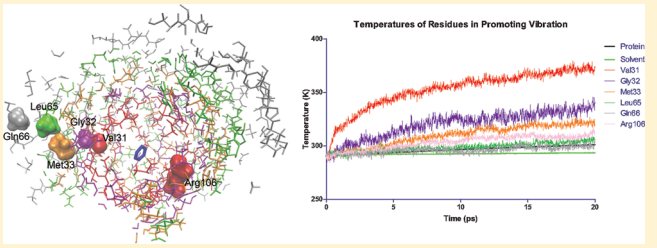

1. INTRODUCTION

The basis for enzymatic catalysis has been widely understood to be enzymatic stabilization of a transition-state intermediary.[1,2] However, recently there has been intense study of the role of dynamics in enzymatic processes. On millisecond time scales, it has been shown that conformational changes in the protein form part of the reaction coordinate.[3,4] Even in catalytic antibodies, the residues near the active site undergo significant motions in the course of the reaction.[5] On shorter time scales, fast picosecond to nanosecond motions play a role in inducing large-scale conformational motions that produce a catalytically competent state.[6] Short time scale motion may also be more intimately involved in the catalytic process.[7,8] In proteins that involve the transfer of a hydrogen species, quantum tunneling effects, as measured by the kinetic isotope effect, surprisingly increase with higher temperatures, whereas one would expect them to decrease if the catalytic site were static.[9,10] These results are consistent with the hypothesis that fluctuations in the protein are directly involved in the reaction coordinate of these enzymes.[11]

Transition path sampling (TPS) studies by our group of the human heart enzyme lactate dehydrogenase (LDH)[12−14] have shown that transition-state residence is very short (70 fs), with a compressional motion through the body of the enzyme a part of the reaction coordinate. In LDH our group was able to identify Val31, Arg106, Gly32, Met33, Leu65, and Gln66 as a key set of amino acids responsible for catalysis.[13] The collected motion of these residues, also known as a promoting vibration (PV), forms a linear axis that compresses the carbonyl oxygen of pyruvate to the NADH donor hydrogen. This compression lowers and thins the barrier for hydride transfer. Quaytman and Schwartz[13] used a commitment probability analysis to identify residues that are part of the reaction coordinate. These residues participate in the PV and in the rest of the paper are designated as PV-Res. We have also shown, using a statistical analysis of the members of the transition-state ensemble, that it is possible to directly identify residues that are part of the reaction coordinate.[14] This method is known as the kernel principal component analysis, and in the rest of the paper these residues are designated as kPCA-Res.

Both methods identify residues through the protein axis. Their similarity can be seen in Figure 3 of ref 14. What has not been established is whether these motions are unique thermal fluctuations in any preferred sense or if they are simply part of the expected thermal motions of the entire body of the protein and not a preferred thermal channel in the enzyme. For example, this case of an important but not preferred direction is what would be obtained in a liquid. The previous calculations do not address this

Received: October 27, 2011
Revised: November 11, 2011
Published: November 14, 2011

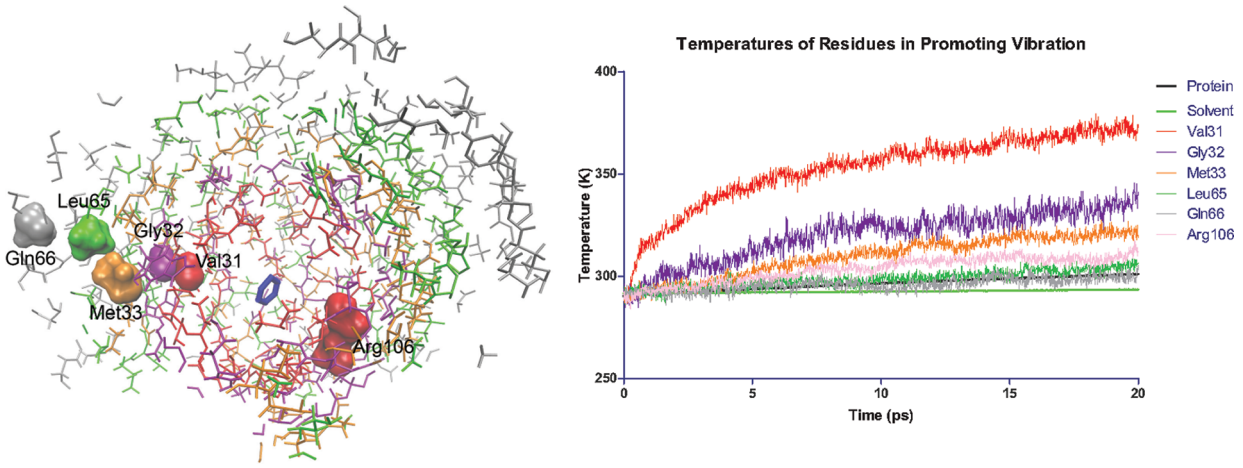

Figure 1. (Left) Different spherical shells containing members of the promoting vibration. Highlighted residues represent the different members of the promoting vibration. (Right) Temperatures of each the residues. Promoting vibration residues closer to the active site maintain higher temperatures throughout the course of the simulation.

question, and it is equally likely that the motions are needed from a mechanistic point of view but are not different than equilibrium fluctuations in the rest of the protein matrix. In this paper we will test whether the promoting vibration is a preferred energy channel by measuring the amount of heat energy flowing through the promoting vibration residues compared to other residues in the protein, as energy analogous to a laser excitation is deposited in the active site.[15] We then study the dynamic structure factor to verify that the direction is preferred within the fluctuation dissipation limit.

Dissipation of heat from the center of a protein is a subject that has been previously studied in myoglobin. Hochstrasser and co-workers[16] first studied the dispersal of heat from the center of myoglobin by exciting the heme moiety in myoglobin with a femtosecond laser. Their experiments show that the majority (60%) of heat flows outward on a time scale (7.5 ps) faster than one predicted by diffusion (20 ps). These results led to the hypothesis that there is ballistic energy transfer through a collective motion that allows heat to reach the solvent more quickly.

Sagnella and Straub[17] et al. replicated the work of Hochstrasser in silico. They confirmed Hochstrasser's result by showing that heat reached solution on a time scale faster than a strictly diffusive process. Using a computational model, Straub and co-workers[18] were able to determine the preferred axis of heat dissipation and show that energy flows preferentially outward in the planar axis of the heme prosthetic group.

Using methods similar to Straub, we will examine anisotropic heat flow in LDH by testing whether energy deposited in the catalytic center flows preferentially outward through the promoting vibration.

2. METHODS

2.1. System Preparation. We used the crystal structure for human heart tetramer LDH solved by Read et al.[19] (PDB file 1I0Z, 2.1 Å resolution). The crystal structure consists of four identical subunits each with 332 residues, an oxamate ligand, and a NADH cofactor. Oxamate (NHCOCOO) is an inhibitor of LDH, similar in structure to pyruvate. In our simulations, the PDB file was modified by replacing the nitrogen atom in oxamate with carbon, in effect substituting the oxamate molecule with a pyruvate. Molecular interactions were calculated by use of the CHARMM27 force field. Parameters for the pyruvate ligand were calculated by methods developed by Mackerell and co-workers[20] as detailed below.

2.2. Pyruvate Parameterization. Pyruvate's geometry was first optimized in Gaussian[21] using MP2[22] to minimize the structure in vacuo. Merz−Kollmann charges, calculated by Gaussian, were used as a starting point for the charge optimization procedure. A single water molecule was added at all potential hydrogen-bond donor/acceptor sites. The geometries of both pyruvate and the water molecule were constrained with the exception of the hydrogen bond donor−acceptor distance. MP2 was used again to minimize the energy of the structure.

The process was repeated in CHARMM, except that the partial charges of the pyruvate atoms were varied empirically until the water interaction energies produced by CHARMM were in good agreement with the ones produced by Gaussian. Next, the dihedral force constant term was calculated. A potential energy scan for the CCCH and the OCCC dihedral bond was calculated in Gaussian. The potential energy scan was matched in CHARMM via a heuristic process where the dihedral constant was manually modified until there was good overlap between the energy scans produced by Gaussian and CHARMM.

2.3. Trajectory Production. Protein dynamics were propagated with the CHARMM force field with a pair calculation distance (cutnb) of 14.0 and a cutoff for where the switching function eliminates the energy contribution of a pair of atoms (ctofnb) of 12.0 . Particle mesh Ewald grid parameters of 128 × 128 × 128 and a Gaussian width parameter $\kappa = 1$ were used.

A preequilibrated 100 Å × 100 Å × 100 Å water box was superimposed over the quaternary protein structure. Any overlapping atoms were deleted and excess charge was neutralized by randomly replacing water molecules with 44 potassium and 12 chloride ions to reach a concentration of approximately 150 mM. The resulting structure was minimized by doing 1000 steepest descent followed by 1000 adopted basis Newton−Raphson minimization (ABNR). A velocity Verlet integration[23] with a time step of 1 fs was used to evolve the system.

The system was slowly heated over 100 ps by reassigning velocities to the system by use of a Berendsen thermostat.[24] The system was allowed to equilibrate for 2 ns in a microcanonical

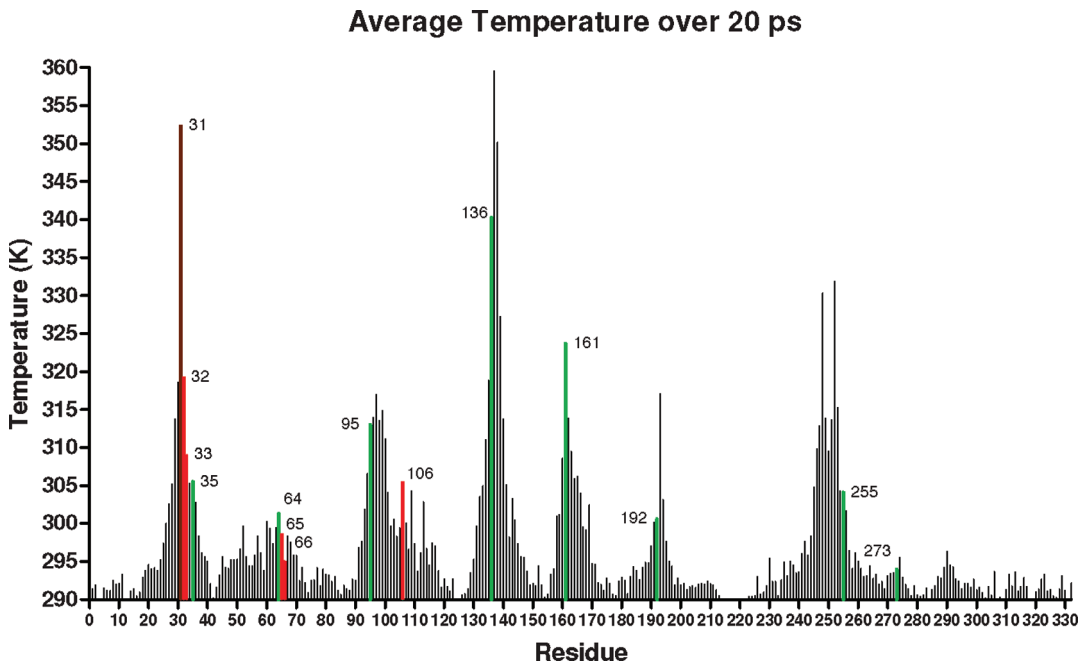

Figure 2. Average temperatures over the 20 ps heating window are shown as spikes. Brown spikes correspond to residues that are both part of the promoting vibration and the kernel PCA residues, red spikes correspond to the promoting vibration residues, and green spikes correspond to kernel PCA residues.

ensemble. During this equilibration the temperature of the system slightly decays from 300 to 290 K as the system reaches an equilibrium state. This is presumably because of redistribution of kinetic energy into the entirety of the vibrational energy space. After equilibration, velocities of atoms in the nicotinamide ring of the four NADH ligands, near the reaction site and what we call the catalytic center, were perturbed 200 times by reassigning their values from a Maxwell−Boltzmann distribution at 1000 K and the system was allowed to propagate for an additional 20 ps to produce independent trajectories. We limited our perturbation to the catalytic center because it disfavors the formation of dramatic conformational changes but at the same time creates the random differences in the positions and velocities necessary for the formation of a statistical ensemble.

The Maxwell−Boltzmann distribution for velocities was calculated by obtaining the product of a Gaussian random variable with the square root of Boltzmann's constant multiplied by the desired temperature divided by the mass of the reassigned atom.

After the initial perturbation and subsequent 20 ps of simulation, the atoms in the nicotinamide rings were then strongly coupled, using a characteristic response time, τ, of 10 000 ps, to a 1000 K Nose-Hoover thermostat. The coupling to the thermostat allows one to continuously inject thermal energy into the reaction center during the simulation. This creates a strong signal that can be followed during the analysis of the data, as opposed to a single excitation that is too weak to be seen during the analysis. Dynamics were then propagated for an additional 20 ps, and the temperatures of the residues were recorded. The temperatures of the residues were then averaged over the 200 individual trajectories for each 1 fs time step.

To calculate the relative temperature of different residues equidistant from the center of heat stimulation, spherical shells were defined at distances of 4−7, 7−10, 10−13, 13−16, 16−19, 19−22, and 22−25 Å. Residues were considered to be part of a given shell if six or more atoms from the residue lie in the shell. Some residues overlapped shells.

Table 1. Rank of Promoting Vibration Residue Temperatures As Compared to Other Residues in the Same Shell[a]

shell	rank of promoting vibration residue	total no. of residues
4−7 Å (31)	2	17
7−10 Å (32)	3	38
10−13 Å (33)	8	46
13−16 Å (33)	1	59
16−19 Å (65)	6	69
19−22 Å (65)	4	75
22−25 Å (66)	6	80

[a] Numbers in parentheses represent the corresponding PV-Res contained in the shell.

3. RESULTS

We heated an ensemble of LDH molecules with pyruvate and NADH bound at the active site of LDH continuously for 20 ps and observed the temperature of residues in successive concentric spherical shells, 3 Å in width, centered at the enzyme's active site. Temperatures of residues that were contained in these shells were compared to determine the preferred anisotropy of energy dissipation. The concentric shells are drawn in the left panel of Figure 1. Also shown in the right panel of Figure 1 is the temperature as a function of time tracing for the promoting vibration residues. As compared to the overall protein and solvent, the promoting vibration residues are significantly hotter.

Figure 2 shows the average temperatures of the residues over the 20 ps heating window. Colored data points in the figure

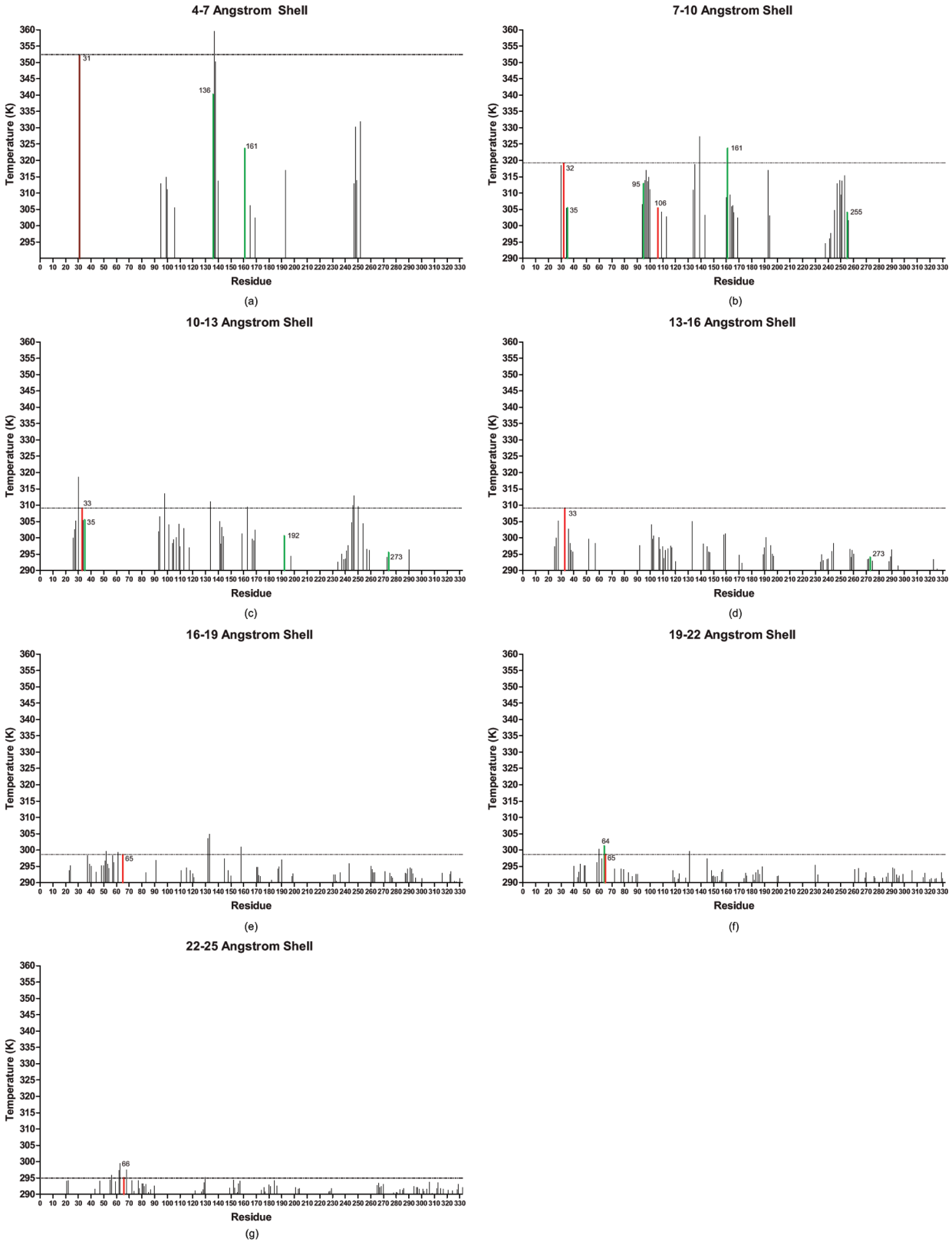

Figure 3. Bar graphs showing the temperatures of all the residues in each concentric 3 Å shell. Residues in red correspond to PV-Res, residues in green correspond to kPCA-Res, and residues in brown correspond to both PV-Res and kPCA-Res. Horizontal lines are drawn from the PV-Res temperatures for aid in visual comparison.

include the promoting vibration residues as identified by Quaytman and Schwartz[13] shown as red spikes, the promoting vibration as identified by the kPCA method[14] shown as green spikes, and residues that are elements of both sets are shown as brown spikes.

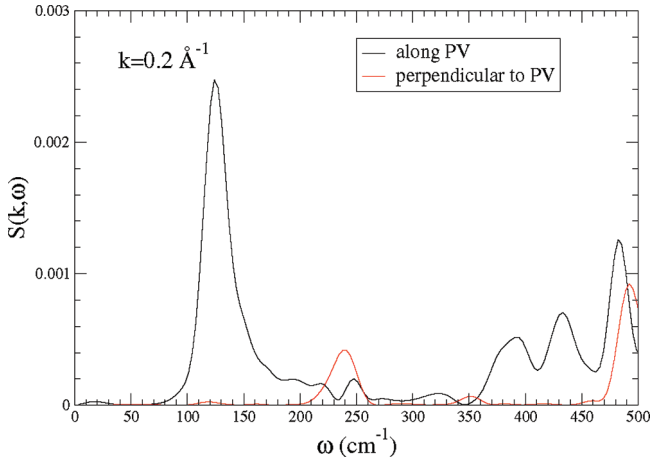

Figure 4. Structure factor $S(\mathbf{k},\omega)$ for k = 0.2 Å^{-1} along the PV axis (black line) and along an axis perpendicular to the promoting vibration. There is strong anisotropy. The sharpness of the peak at 125 cm^{-1} means that there are stable fluctuations along the PV axis for that frequency.

Shells were calculated at 4−7, 7−10, 10−13, 13−16, 16−19, 19−22, and 22−25 Å. Different shells contain different members of the PV-res and kernel PCA promoting vibration residues. Table 1 shows the temperature rank of the promoting vibration residues in each respective shell. Figure 3 shows the temperature of the residues in each respective shell.

Protein residues that are members of the promoting vibration are consistently hotter than most of the other residues equidistant from the center of excitation (Figure 3 and Table 1). The temperatures of residues in concentric spherical shells centered at the heated moiety are compared in Figure 3. Horizontal lines are drawn from PV-Res values in Figure 3 to aid in visual comparison. Quaytman and Schwartz[13] identified members of the promoting vibration as Val31, Arg106, Gly32, Met33, Leu65, and Gln66.

With respect to the promoting vibration residues identified by Quaytman and Schwartz, in each shell the values are as follows. In the 4−7 Å shell, Val31 is on average 29 K or 1.64 standard deviations (SD) hotter than other residues in that shell. In the 7−10 Å shell, Gly32 is on average 10 K or 1.34 SD hotter than other residues in the same shell. Arg106 is 3.9 K or 0.52 SD colder than other residues in the same shell. In the 10−13 Å shell, Met33 is on average 7 K or 1.18 SD hotter than the other residues in the same shell. Met33 overlaps shells and is again found in the 13−16 Å shell. Here it is on average 12 K or 3.34 SD hotter than the other residues. In the 16−19 Å shell, Leu65 is 4.8 K or 1.49 SD hotter than the other residues in the same shell. Leu65 overlaps shells and is again found in the 19−22 Å shell. Here it is on average 5.6 K or 2.3 SD hotter than the other residues. In the 22−25 Å shell, Gln66 is 2.7 K or 1.5 SD hotter than the other residues in the same shell. These values show that the promoting vibration residues are consistently (on average 1.83 SD) hotter than other residues equidistant from the center of excitation.

The residues found by the kernel PCA method correspond closely to the temperature maxima in Figure 2. Significant local maxima are found at residues 31, 97, 137, 161, 193, 248, and 252. The kernel PCA residues 31, 95, 136, 161, 192, and 255 are either identical with or reside very close to the respective local temperature maxima. However, this may be simply secondary to the fact the kernel PCA method residues lie closer to the center of heating. With respect to the kernel PCA residues in each shell, the values are as follows. In the 4−7 Å shell, the temperatures of residues Thr95, Val136, and Ser161 are respectively −10.5 K (−0.59 SD), 16.8 K (0.95 SD), and 0.2 K (0.01 SD) from the mean. In the 7−10 Å shell, the temperatures of residues Cys35, Thr95, and Ser161 are respectively −3.9 K (−0.52 SD), 3.6 K (0.48 SD), and 14 K (1.93 SD) above the mean. In the 10−13 Å shell, the temperatures of residues Cys35 and Glu192 are respectively 3.5 K (0.59 SD) and −1.37 K (−0.23 SD) from the mean. In the 19−22 Å shell, residue Asp64 is 8.2 K (3.51 SD) from the mean. Although some of the kPCA residues are not thermally favored, most are on average (0.68 SD) hotter than other residues equidistant from the center of excitation.

A final question that we examined is why, instead of isotropic vibrational dynamics, there is a preferred direction in LDH. To address this question, we calculated the dynamical structure factor $S(\mathbf{k},\omega)$, defined as the Fourier transform of the density autocorrelation function:

$$S(\mathbf{k},\omega) \equiv \int \mathrm{d}t\, \mathrm{e}^{-i\omega t}\langle \rho_{\mathbf{k}}(t)\rho_{-\mathbf{k}}(0)\rangle = \int \mathrm{d}t\, \mathrm{e}^{-i\omega t} \sum_{i,j} \langle \mathrm{e}^{-i\mathbf{k}\mathbf{r}_i(t)}\mathrm{e}^{+i\mathbf{k}\mathbf{r}_j(0)}\rangle \quad (1)$$

This quantity is also called the coherent dynamical structure factor and is probed, among others, with light scattering experiments. It should not be confused with the incoherent structure factor, which includes only the term $i = j$ in eq 1 and is probed by inelastic scattering experiments. Peaks in the spectrum of $S(\mathbf{k},\omega)$ are associated with sound waves, which are long-lived if the peaks are narrow.[25] Sound waves are long-lived in crystalline solids for all values of k. In amorphous materials like proteins, sound waves are guaranteed to be long-lived provided k is small enough (since small k corresponds to large wavelengths, at a large enough wavelength $S(\mathbf{k},\omega)$ cannot probe the microscopic structure, hence at small enough k all materials are seen as a continuum). In Figure 4 we plot $S(\mathbf{k},\omega)$ for k = 0.2 Å^{-1} (this value of k corresponds to wavelength 31 Å, almost the diameter of LDH), for two directions: along the PV axis and perpendicular to it. We note that along the PV direction there is a stable density fluctuation that is absent in the perpendicular direction, indicating that density fluctuations exhibit an anisotropy, being "softer" along the PV axis. (There an infinity of such possible choices; we randomly choose a variety and always obtained qualitatively similar results.) A possible explanation for the existence of the PV vibration is that for an unrelated reason (e.g., to facilitate folding), it was advantageous for one direction of the protein to be "softer", and the PV vibration is a side effect of this evolved property.

4. CONCLUSION

We have studied the thermal properties of the promoting vibration in hLDH. In our numerical experiments we continuously heated the catalytic center of an ensemble of LDH molecules to 1000 K for 200 independent trajectories initially equilibrated to 300 K. Upon averaging temperature data, we saw that excess kinetic energy dissipates from the heated atoms along an axis corresponding to a previously discovered promoting vibration. The results in Figure 3 show that the residues identified as members of the promoting vibration are preferential carriers of thermal energy. This demonstrates not only that the LDH promoting vibration is a collective protein motion that is

part of the reaction coordinate but also that it forms a preferred channel of energy dissipation. The physical origin is shown through analysis of the dynamic structure factor. The additional role of the promoting vibration as a mechanism for energy redirection is an intriguing result with significant potential biological ramifications.

AUTHOR INFORMATION

Corresponding Author
*E-mail steve.schwartz@einstein.yu.edu.

ACKNOWLEDGMENT

We acknowledge the support of the National Institutes of Health through Grant GM008036 and the National Science Foundation through Grant CHE-0714118.

REFERENCES

(1) Garcia-Viloca, M.; Gao, J.; Karplus, M.; Truhlar, D. G. *Science* **2004**, *303*, 186–195.
(2) Ringe, D.; Petsko, G. A. *Science* **2008**, *320*, 1428–1429.
(3) Boehr, D. D.; McElheny, D.; Dyson, H. J.; Wright, P. E. *Science* **2006**, *313*, 1638–1642.
(4) Bhabha, G.; Lee, J.; Ekiert, D. C.; Gam, J.; Wilson, I. A.; Dyson, H. J.; Benkovic, S. J.; Wright, P. E. *Science* **2011**, *332*, 234–238.
(5) Chen, J.; Deng, Q.; Wang, R.; Houk, K. N.; Hilvert, D. *ChemBioChem* **2000**, *1*, 255–261.
(6) Henzler-Wildman, A., K.; Lei, M.; Thai, V.; Kerns, S. J.; Karplus, M.; Kern, D. *Nature* **2007**, *450*, 913.
(7) Pudney, C.; Hay, S.; Levy, C.; Pang, J.; Sutcliffe, M.; Leys, D.; Scrutton, N. *J. Am. Chem. Soc.* **2009**, *141*, 17072–17073.
(8) Hay, S.; Johanissen, L.; Sutcliffe, M.; Scrutton, N. *Biophys. J.* **2010**, *98*, 121–128.
(9) Kohen, A.; Cannio, R.; Bartolucci, S.; Klinman, J. P. *Nature* **1999**, *399*, 496–499.
(10) Nagel, Z. D.; Klinman, J. P. *Nat. Chem. Biol.* **2009**, *5*, 543–550.
(11) Schwartz, S. D.; Schramm, V. L. *Nat. Chem. Biol.* **2009**, *5*, 551–558.
(12) Basner, J. E.; Schwartz, S. D. *J. Am. Chem. Soc.* **2005**, *127*, 13822–13831.
(13) Quaytman, S. L.; Schwartz, S. D. *Proc. Natl. Acad. Sci. U.S.A.* **2007**, *104*, 12253–12258.
(14) Antoniou, D.; Schwartz, S. D. *J. Phys. Chem. B* **2011**, *115*, 2465–2469.
(15) Nguyen, P. H.; Park, S.-M.; Stock, G. *J. Chem. Phys.* **2010**, *132*, No. 025102.
(16) Lian, T.; Locke, B.; Kholodenko, Y.; Hochstrasser, R. M. *J. Phys. Chem.* **1994**, *98*, 11648–11656.
(17) Sagnella, D. E.; Straub, J. E. *J. Phys. Chem. B* **2001**, *105*, 7057–7063.
(18) Zhang, Y.; Fujisaki, H.; Straub, J. E. *J. Phys. Chem. B* **2007**, *111*, 3243–3250.
(19) Read, J.; Winter, V.; Eszes, C.; Sessions, R.; Brady, R. *Proteins: Struct., Funct., Bioinf.* **2001**, *43*, 175–185.
(20) Vanommeslaeghe, K.; Hatcher, E.; Acharya, C.; Kundu, S.; Zhong, S.; Shim, J.; Darian, E.; Guvench, O.; Lopes, P.; Vorobyov, I.; Mackerell, A. D. *J. Comput. Chem.* **2010**, *31*, 671–690.
(21) Frisch, M. J. et al. Gaussian 09, Revision A.1; Gaussian Inc.: Wallingford, CT, 2009.
(22) Møller, C.; Plesset, M. S. *Phys. Rev.* **1934**, *46*, 618–622.
(23) Lamoureux, G.; Roux, B. *J. Chem. Phys.* **2003**, *119*, 3025–3039.
(24) Berendsen, H. J. C.; Postma, J. P. M.; van Gunsteren, W. F.; DiNola, A.; Haak, J. R. *J. Chem. Phys.* **1984**, *81*, 3684–3690.
(25) Chaikin, P.; Lubensky, T. *Principles of Condensed Matter Physics*; Cambridge University Press: Cambridge, U.K., 1995.